Supporting information (SI) for: Surface charge-induced orientation of interfacial water suppresses heterogeneous ice nucleation on α-alumina (0001)

Ahmed Abdelmonem[1], Ellen H. G. Backus[2], Nadine Hoffmann[1], M. Alejandra Sánchez[2], Jenée D. Cyran[2], Alexei Kiselev[1] and Mischa Bonn[2]

1Institute of Meteorology and Climate Research – Atmospheric Aerosol Research (IMKAAF), Karlsruhe Institute of Technology (KIT), 76344 Eggenstein-Leopoldshafen, Germany
2Max Planck Institute for Polymer Research, Ackermannweg 10, 55128 Mainz, Germany

Correspondence to: Ahmed Abdelmonem (ahmed.abdelmonem@kit.edu)

Effect of ionic strength on freezing temperature

To confirm that the ionic strength, which changes as well when changing the pH, is not influencing the freezing temperature, cold stage experiment were performed for water and 10^{-5} and 10^{-3} M NaCl solutions. As is clear from Fig. S1, the freezing temperature is not significantly varying. Please note that the freezing temperature for pH7 is now slightly lower than the one reported in Fig. 1 of the manuscript due to slightly different droplet sizes in the two (pH– and salt concentration–dependent) different sets of experiments.

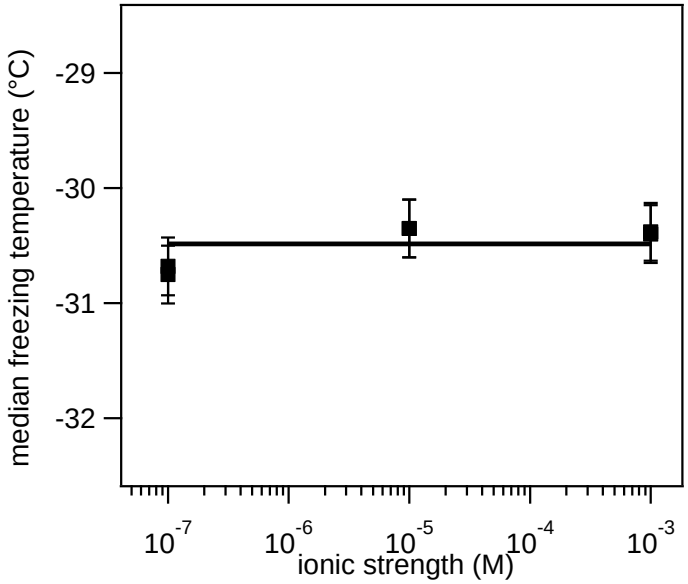

Figure S1. Median freezing temperature at sapphire 0001 as function of ionic strength

SFG experiments

The SFG experiments are carried out in a co-propagating, total internal reflection geometry from the prism side to avoid strong absorption of the infrared light by vibrations of the liquid. Both beams hit the prism very close to the

surface normal to minimize dispersion effects. The setup is similar to the two-beam SHG setup described in (Abdelmonem et al., 2015), however one of the two visible beams is replaced by a broad band IR beam (BB-IR) covering the OH vibrations. These infrared pulses were generated by an OPG/OPA (TOPAS, Light Conversion) system pumped by another part of the 800 nm output of the laser system. The infrared pulses have an energy of ~1.5 μJ and cover the range between 3000 and 3900 cm^{-1}. In order to minimize the absorption of the infrared pulses by water vapor, the path of the IR beam is continuously purged with N_2 gas. The narrow-band visible beam providing the frequency resolution in the SFG experiment, was obtained by passing part of the output of a 100 fs amplified Ti:sapphire laser system (Spitfire Ace, SpectraPhysics) through an etalon. The visible beam has a central wavelength of ~800 nm, an energy of ~25μJ at 1 kHz with a full width half maximum bandwidth of 20 cm^{-1}. The generated SFG light, in reflection geometry, is spectrally dispersed by a monochromator (Acton 300i) and detected by an electron-multiplied-charge-coupled-device (EMCCD, Andor Technologies). The acquisition time is set to 30 s per spectrum. We cool the sample stepwise with a rate of 1 °C/min and a step size of 1 °C. We let the system equilibrate at each step and then collect a spectrum. The spectra of the water/sapphire change slightly and gradually with cooling (primarily due to temperature dependent optical constants). At the transition point, a significant change in the signal is observed on the CCD camera and, simultaneously, visual inspection reveals that the droplet is frozen. The spectra of liquid and ice we discuss here are those collected right before (liquid) and immediately after (ice) the freezing of the droplet, respectively. A collected spectrum is either of pure liquid or pure ice. To correct for the frequency spectrum of the IR pulse, the SFG spectra are normalized to the signal from gold. To this end, an identical sapphire prism was coated with a 100 nm gold film at its hypotenuse and the nonresonant (NR) SFG intensity from the sapphire/gold interface was recorded as a function of temperature in the same frequency and temperature ranges applied in this study. The dependence of the NR signal at the sapphire/gold interface on temperature was found to be negligible compared to the changes in SFG signal at the sapphire/water (ice) interface particularly at the point of the phase change. All signals were collected under SSP (s-polarized SFG output, s-polarized visible input, and p-polarized IR input) polarization combination.

Data analysis and Fresnel factors

The SFG signal with frequency $\omega_{SF} = \omega_v + \omega_{IR}$ under SSP polarization generated at the spatial and temporal overlap of the incoming visible with frequency ω_v and infrared light with frequency ω_{IR} can be described with the equation:

$$S_{SSP}(\omega_{SF}) \propto \left| L_{yy}(\omega_{SF}) L_{yy}(\omega_v) L_{zz}(\omega_{IR}) \chi^{(2)}_{yyz} \right|^2 I_v I_{IR} \quad (1)$$

where, $L(\omega_i)$ is the Fresnel factor at ω_i and $\chi^{(2)}_{yyz}$ is the surface nonlinear susceptibility tensor for SSP polarisation. To obtain the molecular quantity $\chi^{(2)}_{yyz}$ the measured SFG spectra have thus to be corrected for the Fresnel factors. As the SFG and visible Fresnel factor are frequency independent and within 10% the same for ice and water, we ignore their contribution. The frequency dependent IR Fresnel factor is calculated following(Zhuang et al., 1999) using the refractive index of H_2O for the interfacial refractive index (Backus et al., 2012). Unfortunately, the refractive index of ice and liquid water are only reported in literature for specific temperatures. We use the refractive index of liquid

water at -20°C which is close to our experimental temperature in the SFG experiment (Zasetsky et al., 2005). For ice we use the value reported by the same author at -38 °C, which is the closest to the experimental conditions (Zasetsky et al., 2005). The refractive index of Sapphire is calculated from Sellmeier equation (Dodge, 1986). The spectra reported in Figure 3 are the Fresnel corrected ones and are thus directly proportional to $\left|\chi^{(2)}_{yyz}\right|^{(2)}$.

To obtain peak frequencies and amplitudes the $\left|\chi^{(2)}_{yyz}\right|^{(2)}$-spectra were fit with a sum of a non-resonant contribution, with amplitude A_0 and phase φ, and a sum of Lorentzian peaks for the resonant contribution:

$$\left|\chi^{(2)}_{yyz}\right|^{(2)} = \left|\chi^{(2)}_{NR} + \chi^{(2)}_{R}\right|^{(2)} = \left|A_0 e^{i\varphi} + \sum_q \frac{A_q}{\omega_{IR} - \omega_q + i\Gamma_q}\right|^{(2)} \quad (2)$$

where A_q, ω_q, and $2\Gamma_q$ are the amplitude, frequency, and full width half maximum linewidth of the q^{th} vibrational resonance, respectively.

REFERENCES

Abdelmonem, A., Lützenkirchen, J., and Leisner, T.: Probing ice-nucleation processes on the molecular level using second harmonic generation spectroscopy, Atmos. Meas. Tech., 8, 3519-3526, doi: 10.5194/amt-8-3519-2015, 2015.

Backus, E. H. G., Garcia-Araez, N., Bonn, M., and Bakker, H. J.: On the Role of Fresnel Factors in Sum-Frequency Generation Spectroscopy of Metal–Water and Metal-Oxide–Water Interfaces, The Journal of Physical Chemistry C, 116, 23351-23361, doi: 10.1021/jp306273d, 2012.

Dodge, M. J.: Refractive Index, in: Handbook of Laser Science and Technology, edited by: Weber, M. J., Laser & Optical Science & Technology, 2, CRC Press, Boca Raton, 30, 1986.

Zasetsky, A. Y., Khalizov, A. F., Earle, M. E., and Sloan, J. J.: Frequency Dependent Complex Refractive Indices of Supercooled Liquid Water and Ice Determined from Aerosol Extinction Spectra, The Journal of Physical Chemistry A, 109, 2760-2764, doi: 10.1021/jp044823c, 2005.

Zhuang, X., Miranda, P. B., Kim, D., and Shen, Y. R.: Mapping molecular orientation and conformation at interfaces by surface nonlinear optics, Physical Review B, 59, 12632-12640, doi: 10.1103/PhysRevB.59.12632, 1999.